

Influence of temper condition on microstructure and mechanical properties of semisolid metal processed Al–Si–Mg alloy A356

H. Möller^{*1}, G. Govender¹, W. E. Stumpf² and R. D. Knutsen³

The microstructures and mechanical properties of strontium modified semisolid metal high pressure die cast A356 alloy are presented. The alloy A356-F (as cast) has a globular primary grain structure containing a fine eutectic. Solution treatment results in spheroidisation of the eutectic silicon particles under the T4 and T6 temper conditions. The A356-T5 maintains the fibrous silicon morphology after artificial aging. A356-T4 has better ductility and impact strength than A356-T5 due to its spheroidised silicon morphology. The impact properties of semisolid metal high pressure die cast A356 are controlled mainly by the silicon morphology and alloy strength (hardness), whereas tensile strength is determined by the degree of solid solution coupled with precipitate formation during aging.

Keywords: Semisolid metal forming, Alloy A356, Mechanical properties, Temper conditions, Impact properties

Introduction

Semisolid metal (SSM) processing is a manufacturing method capable of producing near net shape products for various industrial applications.¹ A semisolid structure (free of dendrites) is produced with the solid alloy particles present in a near spherical form. This semisolid mixture flows homogeneously, behaving as a thixotropic fluid with viscosity depending on the shear rate and fraction of solid in the liquid, either by thixocasting or rheocasting. With thixocasting, a specially prepared billet of solid material with a globular microstructure is reheated into the semisolid range, followed by a forming process, such as high pressure die casting (HPDC). With rheocasting, an SSM slurry is prepared directly from the liquid, followed by HPDC. The higher costs associated with thixocasting have resulted in rheocasting becoming the preferred semisolid process. The laminar flow provided by SSM processing during the die fill prevents the problems of oxide and gas entrapment and also reduces the shrinkage problems during solidification.² Blistering during subsequent heat treatment can, therefore, be prevented.^{3–7}

The conventional casting Al–Si–Mg alloy A356 is probably the most popular alloy used for SSM forming. This is due to its high fluidity and good ‘castability’.⁸ In

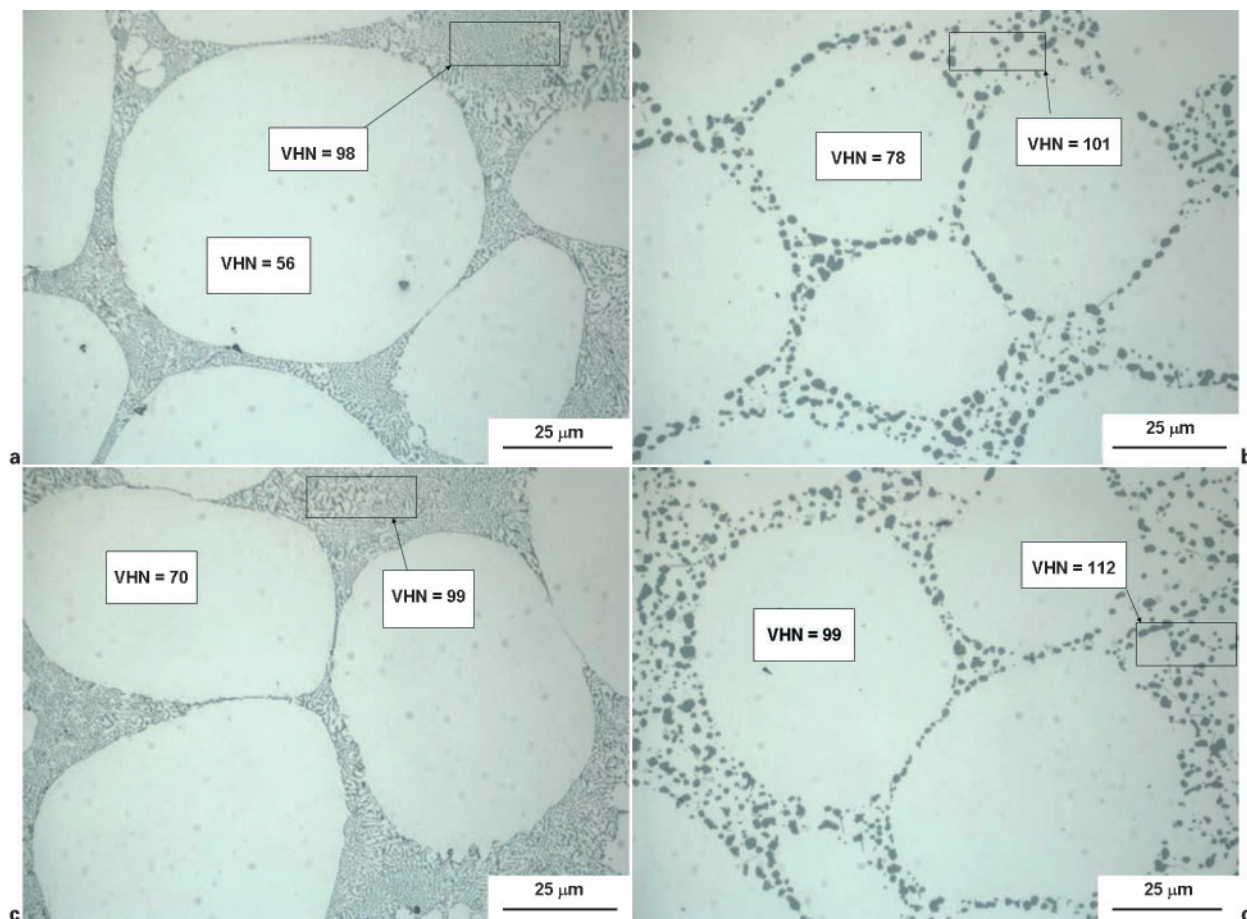
Sr modified SSM-HPDC A356, the microstructure under the as cast condition (F temper) consists of globular α -Al and a fine eutectic with fibrous silicon particles.^{3–6} Spheroidisation of these silicon particles occurs during solution treatment of the alloy, which leads to improved ductility. Natural aging (for at least five days at room temperature after the solution treatment and water quench) results in the T4 temper.⁵ The natural aging response is considered to be due to the formation of (Mg+Si) clusters and Guinier–Preston zones.⁹ The T5 temper⁷ is achieved by artificially aging the as cast material without a solution treatment, in contrast with the T6 temper condition⁵ where a solution treatment is used. The advantages of not using a solution treatment include significant energy savings and less distortion of the components. However, spheroidisation of the silicon particles is not achieved under the A356-T5 condition.^{7,10} Lower strength is also obtained in A356-T5 than in A356-T6 due to less supersaturation of strengthening solutes before artificial aging. Hardening with artificial aging (from the T5 and T6 tempers) occurs from the precipitation of the metastable and coherent β'' (Mg₂Si) and semicoherent β' (Mg₂Si) phases.^{9,10} The mechanical properties and microstructures of conventionally cast (dendritic) A356 under different temper conditions have been reported by Caceres and Barresi.¹¹ The objective of this study was to characterise the microstructural changes that occur in rheocast (globular) A356-F when it is heat treated to the T4, T5 and T6 tempers respectively. The concurrent changes in mechanical properties (hardness, yield strength, ultimate tensile strength, per cent elongation and impact strength) are also reported.

¹Materials Science and Manufacturing, CSIR, Meiring Naude Road, Brummeria, Pretoria, Gauteng, 0001, South Africa

²Department of Materials Science and Metallurgical Engineering, University of Pretoria, Pretoria, South Africa

³Centre for Materials Engineering, University of Cape Town, Cape Town, South Africa

*Corresponding author, email hmoller@csir.co.za



1 Light micrographs of SSM-HPDC *a* A356-F indicating globular primary α -grains in fibrous Si- α eutectic matrix, *b* A356-T4 indicating modified eutectic structure (spheroidised Si) after solution treatment, *c* A356-T5 indicating retained fibrous Si- α eutectic matrix and *d* A356-T6 indicating similar structure to A356-T4 condition (note that β' and β'' precipitates cannot be resolved at this magnification)

Experimental

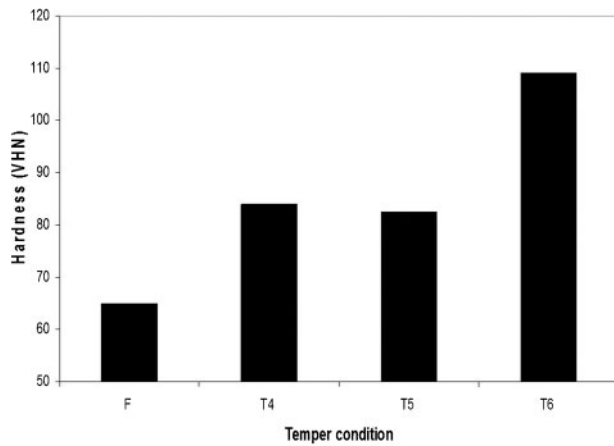
Semisolid metal slurries of A356, whose chemical composition is Al–7.08Si–0.38Mg–0.10Fe–0.12Ti–0.02Sr–0.01Cu–0.01Mn–0.01Zn (wt-%), were prepared using the Council for Scientific and Industrial Research rheocasting process.¹² Plates (4 × 80 × 100 mm) were cast in steel moulds with a 50 t HPDC machine. The heat treatment parameters used to achieve different temper conditions (temperatures and times) were optimised by the authors, and these results are shown elsewhere.^{3–7} For the T4 and T6 temper conditions, solution treatment was performed at 540°C for 1 h, followed by a water quench (20°C). The T6 treated samples were then naturally aged for 20 h, before artificial aging for 4 h at 180°C. The T4 treated samples were allowed to naturally age (at 25°C) for at least 120 h. The samples used for the T5 temper condition were quenched in water after SSM-HPDC and naturally aged for 120 h before artificial aging at 180°C for 4 h. To get an indication of the supersaturation that is obtained for the T5 temper after quenching, ProCAST software was used to determine how the plates cool down in the die during the intensification step. Values of $T_{\text{initial}}=580^{\circ}\text{C}$ (casting temperature) and $T_{\text{die}}=250^{\circ}\text{C}$ were used for the simulation. The results revealed that the temperature of the plates were $\sim 300^{\circ}\text{C}$ after intensification for 30 s before quenching in water.

All samples were etched with 0.5% hydrofluoric acid solution for light microscopy examination in bright field mode. The tensile properties of the samples were determined using tensile samples (substandard size)³ that were machined from the plates. A total of five tensile tests were used for each heat treatment condition. The impact properties were determined by a drop weight test using three substandard size Charpy specimens (55 × 10 × 3 mm with a 45° notch of 2 mm depth) for each temper condition. The mass of the weight for the drop weight test was 5.5 kg. In order to achieve a total projectile energy of 5 J, a drop height of 9.28 cm was required. This resulted in a speed at impact of 1.35 m s⁻¹.

Results and discussion

Light microscopy and Vickers microhardness

Light micrographs of SSM-HPDC A356 are shown in Fig. 1 for the as cast condition or F temper (Fig. 1*a*), T4 temper (Fig. 1*b*), T5 temper (Fig. 1*c*) and the T6 temper (Fig. 1*d*). The average Vickers microhardness (100 g load) values (from eight measurements) of the α -Al and eutectic under all temper conditions are also shown in Fig. 1. Heat treatment to the T4 and T5 temper conditions results in an increase in the hardness of the α -Al grains relative to the A356-F condition. Hardening in A356-T4 occurs due to Guinier–Preston zones and



2 Vickers macrohardness of SSM-HPDC A356 under different temper conditions

solute clusters, whereas in A356-T5, β'' and β' precipitation occurs.⁹ Solid solution strengthening under A356-T4 condition should also be more significant than that under the T5 temper condition. In A356-T6, the volume fraction of β'' ought to be much higher than in A356-T5 (due to the solution treatment), and the resultant hardness is also significantly higher.

The microstructural changes observed in Fig. 1 due to heat treatment are typical for Sr modified SSM-HPDC A356.^{3–6} The fibrous silicon particles in A356-F are spheroidised by the solution treatment applied on A356-T4 (Fig. 1b) and A356-T6 (Fig. 1d). For A356-T5, no solution treatment is used, and it is seen from Fig. 1c that the artificial aging temperature is too low to cause any spheroidisation of the eutectic silicon particles.

Vickers macrohardness

The Vickers macrohardness (20 kg) was also determined (eight measurements/temper conditions), and the results are shown in Fig. 2. In this case, the larger hardness indentation measures the combined hardness of the primary α grains and the matrix.

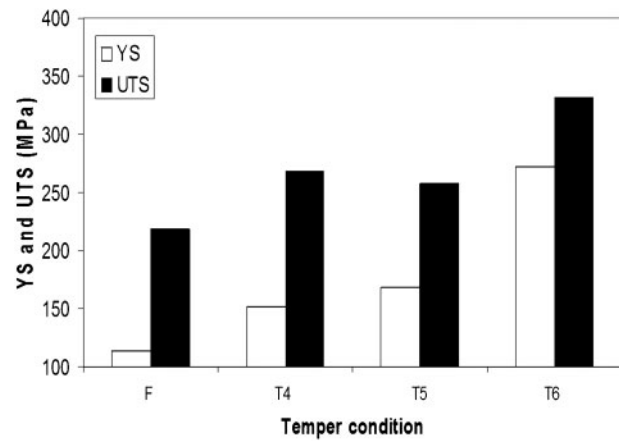
Tensile properties of SSM-HPDC A356

The tensile properties of the A356 under different temper conditions were determined. These results are shown in Table 1 and highlighted in Fig. 3. The importance of the solution treatment in dissolving all the solutes for precipitation hardening during artificial aging can clearly be seen by comparing the lower tensile properties of A356-T5 than A356-T6. On the other hand, the beneficial effect of artificial aging after solution treatment (A356-T6) rather than natural aging (A356-T4) is also evident.

Table 1 Yield strength (YS), ultimate tensile strength (UTS), per cent elongation and quality index (QI) of heat treated samples*

Temper	YS, MPa	UTS, MPa	Per cent elongation	QI, MPa
F	113 (3.0)	218 (2.5)	10.6 (1.6)	372
T4	152 (2.1)	268 (3.9)	14.5 (1.4)	442
T5	168 (2.2)	258 (4.0)	8.4 (0.9)	396
T6	272 (5.1)	332 (4.4)	7.9 (1.5)	466

*The standard deviation for tensile properties (from five samples/temper conditions) is also indicated in brackets.



3 Tensile properties for SSM-HPDC A356 under different temper conditions

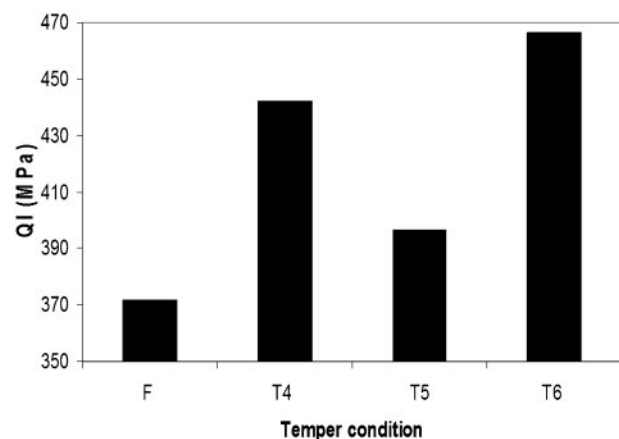
The quality index (QI) relates the strength and ductility (ultimate tensile strength or UTS) into a single term. It was originally developed by Drouzy *et al.*¹³ based on the observation of trends in empirical data. However, Caceres *et al.*¹⁴ have shown the fundamental basis of the QI. Shivkumar *et al.*¹⁵ used the QI to optimise the heat treatments of dendritic A356. The QI (specifically for alloy A356) is given by equation (1)^{13–15}

$$QI \text{ (MPa)} = UTS \text{ (MPa)} + 150 \times \log(\% \text{ elongation}) \quad (1)$$

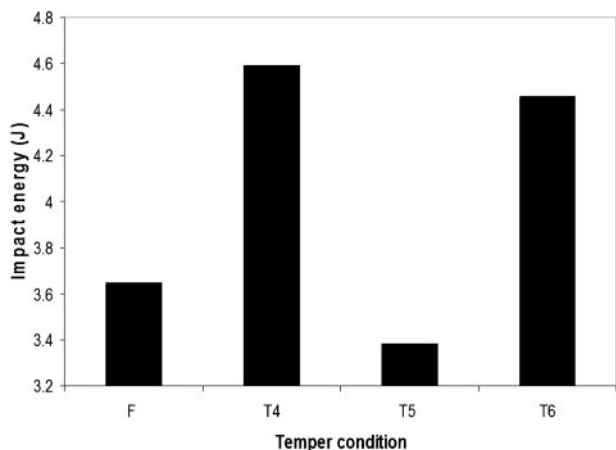
The rationale behind this equation lies in the known phenomenon that, for most mechanisms of strengthening in alloys (except for grain refinement), one has to sacrifice some ductility or toughness. A high QI aims to find a combination of high strength and high ductility or toughness in the alloy. The QI for SSM-HPDC alloy A356 under different temper conditions is shown in Table 1 and highlighted in Fig. 4. It is seen that the high ductility of A356-T4 and high strength of A356-T6 result in high QI values for these two temper conditions in comparison to the F and T5 conditions.

Impact properties of SSM-HPDC alloy A356

The impact energies for A356 under different temper conditions are shown in Fig. 5. Alloy strength (hardness, Fig. 2) and silicon morphology (Fig. 1) have the biggest effects on the impact properties of this material. The



4 Quality index values for SSM-HPDC A356 under different temper conditions



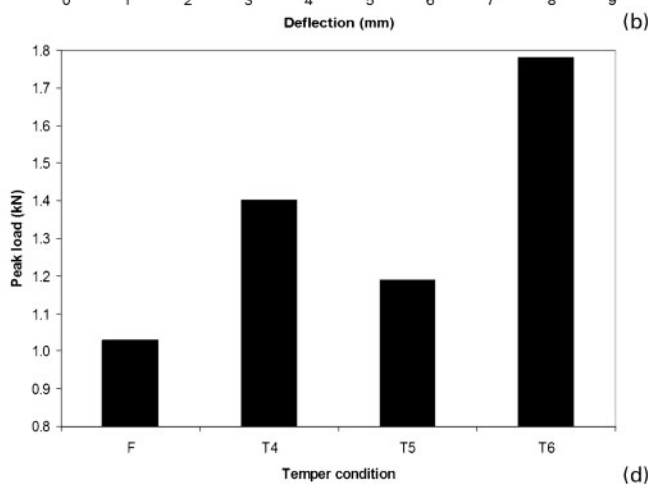
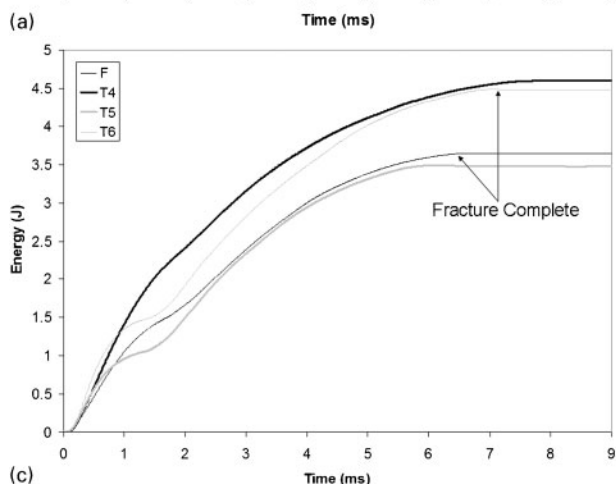
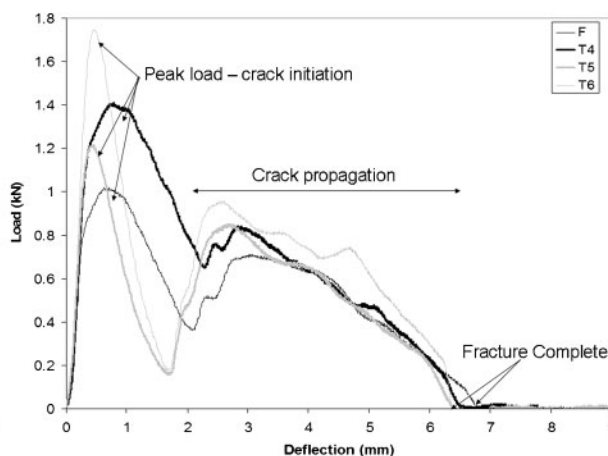
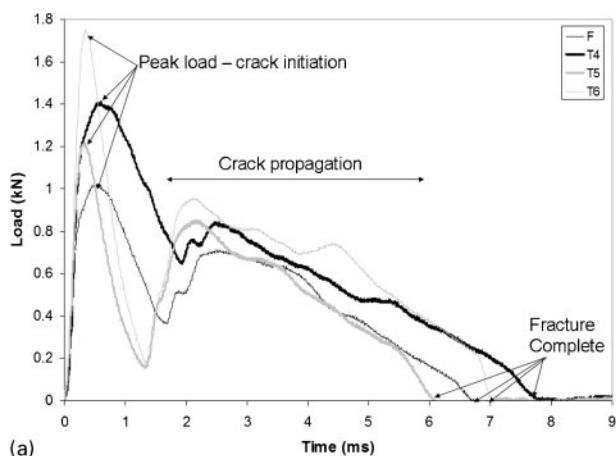
5 Drop weight impact energies for SSM-HPDC A356

influence of hardness of the alloys on the impact properties can be determined by comparing temper conditions under which the silicon morphologies are similar. In both A356-T4 and A356-T6, spheroidised silicon is found (Fig. 1b and d). However, the impact strength of the material is slightly higher for A356-T4 than A356-T6. This difference can be related to the lower hardness of the material under the T4 condition compared to the T6 condition (see Fig. 2 and also that the Vickers microhardness of the α -Al is only 78 HV for the T4 condition compared to 99 HV for the T6 condition in Fig. 1). In both A356-F and A356-T5, fibrous silicon is found (Fig. 1a and c). Again, the

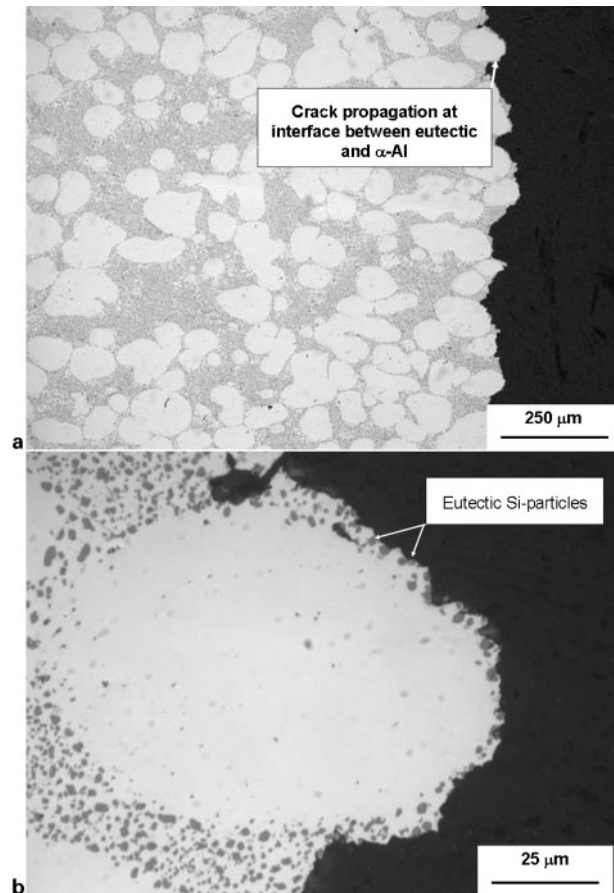
impact strength of the material is slightly higher for the lower hardness A356-F than A356-T5 (see Fig. 2 and also that the Vickers microhardness of the α -Al is only 56 HV for the F condition compared to 70 HV for the T5 condition in Fig. 1). Crack propagation is more difficult in softer materials due to blunting, resulting in better impact properties.

The influence of silicon morphology on the impact properties can be determined by comparing temper conditions under which the silicon morphologies are different (and considering the differences in hardness, too). The impact strength of A356-F and A356-T5 (with fibrous Si) is significantly lower than that of A356-T4 and A356-T6 (with spheroidised Si). This is in spite of the fact that the hardness values of A356-F and A356-T5 are lower than that of A356-T4 and T6 (Figs. 1 and 2). As was shown before, the lower hardness of A356-F and T5 compared to A356-T4 and T6 should actually have a beneficial effect on their impact properties. The observed lower impact strengths of A356-F and T5 compared to A356-T4 and T6 are, therefore, related to the fibrous silicon particles. The tips of fibrous silicon particles most likely act as stress concentrators causing much lower impact strengths than when the silicon particles are spheroidised.

The impact load as a function of time was measured and is presented in Fig. 6a. The first peak (maximum load) in Fig. 6a corresponds to crack initiation, whereas the rest of the curve corresponds to crack propagation. The total time to complete fracture (time-to-zero load in Fig. 6a) is longer for T4 compared to T6 and F



6 a impact load as function of time, **b** impact load as function of deflection, **c** impact energy as function of time (fracture is complete once lines become horizontal) and **d** peak load measured during drop weight testing of SSM-HPDC A356



7 a fracture path in SSM-HPDC A356-T6 tensile specimen (cross-section of tensile fracture surface) and b higher magnification micrograph showing fracture bypassing α -Al in SSM-HPDC A356-T6 tensile specimen

compared to T5. This confirms that crack propagation occurs more rapidly in the harder materials. The impact load as a function of deflection is shown in Fig. 6b. The total energy (Fig. 5) is the area beneath this load versus deflection curve. The impact energy as a function of time is shown in Fig. 6c. The narrow peak widths of the T5 and T6 temper conditions (Fig. 6a and b) result in the inflection points at ~ 1.5 ms in Fig. 6c. The peak load value (Fig. 6d) for the T6 condition is higher than that for the T4 condition, but the width of the peak is narrower. This is most likely due to the higher hardness (strength) of the T6 material, requiring a higher impact load to initiate the crack. However, after crack initiation, its propagation is much easier through the harder material, causing the narrow peak width compared to the softer T4 material. A similar mechanism is operative when comparing the T5 and F (both with fibrous silicon) temper conditions.

Tensile and impact test fracture surfaces

The cross-section of the fracture surfaces of the tensile and impact tested samples were studied using light microscopy. It was found that the fracture paths for the different tests under the different temper conditions

were fairly similar, and therefore, only the results of A356-T6 are presented. Figure 7a shows that the crack propagates preferentially through the eutectic regions and not through the softer α -Al globules. Figure 7b shows a higher magnification micrograph where the fracture completely bypassed an α -Al grain.

Conclusions

1. The hardness values of SSM-HPDC A356 under the T4 and T5 temper conditions are relatively similar. However, the A356-T4 has better ductility and impact strength than A356-T5 due to its spheroidised silicon morphology.

2. The impact properties of SSM-HPDC A356 are controlled mainly by silicon morphology and, to a lesser extent, by hardness (strength). Spheroidised silicon particles (in combination with lower hardness) result in improved impact properties.

3. The solution treatment of alloy A356 has a dual beneficial effect: it causes spheroidisation of the eutectic silicon particles (improved ductility and impact properties), and it causes complete dissolution of the strengthening solutes (maximum strength after artificial aging). Consequently, the added cost of implementing the T6 heat treatment is justified in optimising a good combination of impact and tensile properties.

Acknowledgements

The contributions of D. Wilkins, C. McDuling and A. Grobler are gratefully acknowledged, as well as financial support from the Department of Science and Technology in South Africa.

References

1. H. V. Atkinson: *Prog. Mater. Sci.*, 2005, **50**, 341–412.
2. W. L. Winterbottom: *Metall. Sci. Technol.*, 2000, **18**, 5–10.
3. H. Möller, G. Govender and W. E. Stumpf: *Int. J. Cast Met. Res.*, 2007, **20**, 340–346.
4. H. Möller, G. Govender and W. E. Stumpf: *Open Mater. Sci. J.*, 2008, **2**, 6–10.
5. H. Möller, G. Govender and W. E. Stumpf: *Open Mater. Sci. J.*, 2008, **2**, 11–18.
6. H. Möller, G. Govender and W. E. Stumpf: *Solid State Phenom.*, 2008, **141–143**, 737–742.
7. H. Möller, G. Govender and W. E. Stumpf: *Mater. Sci. Forum*, 2009, **618–619**, 365–368.
8. D. Liu, H. V. Atkinson, P. Kapranos, W. Jirattiticharoen and H. Jones: *Mater. Sci. Eng. A*, 2003, **A361**, 213–224.
9. A. K. Gupta, D. J. Lloyd and S. A. Court: *Mater. Sci. Eng. A*, 2001, **A301**, 140–146.
10. B. Dewhirst, D. Apelian and J. Jorstad: *Die Cast. Eng.*, 2005, **49**, 38–44.
11. C. H. Caceres and J. Barresi: *Int. J. Cast Met. Res.*, 2000, **12**, 377–384.
12. L. Ivanchev, D. Wilkins and G. Govender: Proc. 8th Int. Conf. on ‘Semi-solid processing of alloys and composites’, Limassol, Cyprus, September 2004, WPI’s Metal Processing Institute, Paper 152.
13. M. Drouzy, S. Jacob and M. Richard: *AFS Int. Cast Met. Res. J.*, 1980, **5**, 43–50.
14. C. H. Caceres, M. Makhoulouf, D. Apelian and L. Wang: *J. Light Met.*, 2001, **1**, 51–59.
15. S. Shivkumar, S. Ricci, B. Steenhoff, D. Apelian and G. Sigworth: *AFS Trans.*, 1989, **138**, 791–810.